UNSUPERVISED CHANGE DETECTION ON MULTI-TEMPORAL SATELLITE IMAGES USING TENSOR DECOMPOSITION LEARNING

Anastasia Aidini [1], *Grigorios Tsagkatakis* [1,2], *Panagiotis Tsakalides* [1,2]

[1] Institute of Computer Science, Foundation for Research and Technology-Hellas (FORTH), Greece
[2] Department of Computer Science, University of Crete, Greece

ABSTRACT

The substantial volume of continuously gathered remote sensing data can serve as a valuable information source in mitigating the effects of natural disasters. This involves identifying changes in the time series of observations. Considering that the precise location of the changes may not be available in real-world scenarios, we propose an unsupervised method for detecting extreme events in multi-temporal satellite images. Specifically, we learn a basis matrix of each dimension of the feature space of the images using the tensor decomposition learning method. Then, each new image is represented in the feature space by expressing it as a multilinear combination of the learned tensor decomposition factors. The predicted changes can be obtained by comparing and thresholding the distance of the corresponding extracted features of the images before and after the event. Experimental results on real Sentinel-2 multi-temporal images demonstrate that the proposed method can efficiently detect the effects of fires and floods with low complexity.

Index Terms— Unsupervised change detection, Tensor decomposition learning, Multi-temporal data, Feature space

1. INTRODUCTION

Remotely sensed imagery has been widely used in various Earth Observation applications, including disaster assessment [1], land cover change detection, and environmental monitoring [2]. In particular, remote sensing has proven to be a powerful tool for monitoring and assessing the impacts of extreme events such as floods, droughts, heatwaves, wildfires, cyclones, and landslides. Satellite data from multiple sources can contribute to providing timely and accurate spatio-spectral observations to effectively detect extreme events by identifying changes in the images, contributing to a better understanding of their formation, development, and associated impacts.

Several change detection methods have been developed and applied to satellite images utilizing observations from the same location captured at different time instances. However, the location of the true changes is not available in practical applications. Addressing this issue, unsupervised approaches employ pixel-by-pixel analysis to generate a difference image. This is based on the assumption that changes result in noticeable differences in pixels. Specifically, the distribution of the difference image is used in [3–5], and a spatio-spectral band expansion technique for the introduction of more distinct structural information is presented in [6]. A band-by-band processing approach is proposed in [7], while the Bayesian framework is used in [8] to remove noise from changed pixels and minimize the rate of false alarms. Another approach proposed in [9] is based on image reconstruction loss, using the source and the associated photometrically transformed images.

In recent years, several deep learning-based methods have been introduced to detect changes in bi-temporal satellite images. Specifically, a convolutional neural network for semantic segmentation is proposed in [10] to extract compressed image features and classify the detected changes into the associated semantic classes. Deep neural networks are also introduced in [11, 12] for feature extraction. Another method outlined in [13] utilizes a Generative Adversarial Network to generate additional images, thereby providing more accurate predictions. Finally, [14] introduces a change detection method that integrates graph-based and deep learning techniques within a multi-temporal context.

At the same time, tensor-based methods have showcased the capability to aptly represent the structural characteristics of high-dimensional data, yielding notable results across various problems [15]. In the context of the change detection problem, it has been demonstrated that Tucker decomposition can simultaneously suppress the difference of unchanged pixel pairs and amplify the difference of changed pixel pairs [16]. Specifically, the authors in [16] use Tucker decomposition and high-order principal component extraction to mitigate the impact of various factors in bi-temporal images. Another approach has been introduced in [17] using the tensor train decomposition to capture global correlations from tensors and extract low-rank discriminative features.

Despite their success, the aforementioned methods focus on detecting changes in bi-temporal remote sensing imagery,

This work was supported by the TITAN ERA Chair project (contract no. 101086741) within the Horizon Europe Framework Program of the European Commission.

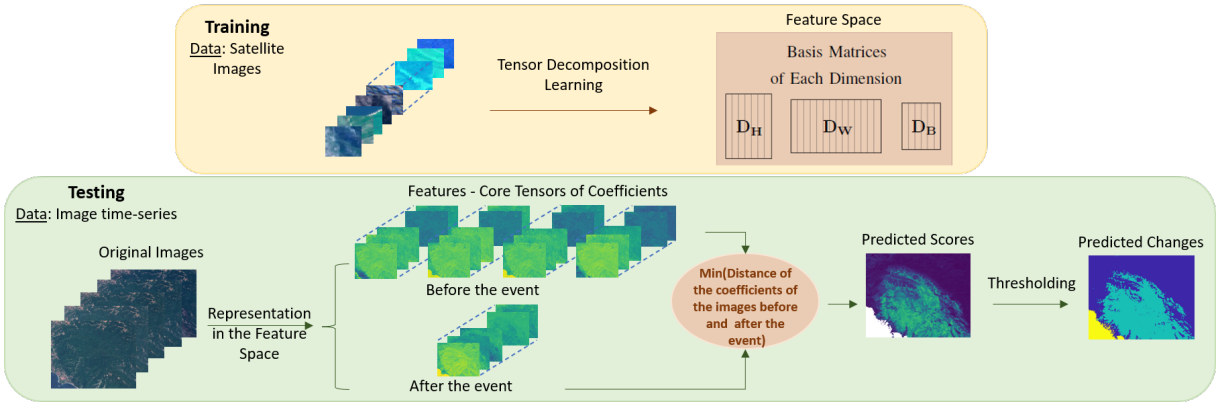

Fig. 1: Flowchart of the proposed unsupervised change detection method. During training, available satellite data is utilized to learn the feature space using the tensor decomposition learning method. In the inference phase, each image is represented in the feature space by expressing it as a multilinear combination of the acquired basis matrices. Predicted changes are then determined by comparing and thresholding the distance of the extracted features from the images before and after the event.

underutilizing the wealth of available observations. To our knowledge, the RaVÆn method, as introduced in [18], is the only one applied to multi-temporal data. This method utilizes a variational autoencoder to generate a latent representation of incoming sensor data within a specific region.

In this work, we propose an unsupervised change detection method for extreme events in multi-temporal satellite images using tensor decomposition learning. Specifically, we learn a basis matrix of each dimension of the feature space of the images using Tucker decomposition. Given the learned decomposition matrices, each new image in the time series is represented in the feature space by expressing it as a multilinear combination of the learned basis matrices. To identify the changed pixels in the images and detect the effects of extreme events, we compare the corresponding coefficients of the images before and after the event. This is done using the Spectral Angle Mapper as a distance metric, taking the minimum distance along the coefficients of the images before the event, as depicted in Fig. 1. The proposed tensor learning model can simultaneously exploit the spatial and spectral features with low complexity, and deal with multi-temporal multispectral images to achieve improved performance, as is demonstrated in the detection of fires and floods.

Overall, the key contributions of this paper can be summarized as follows:

- A novel unsupervised change detection method is proposed to detect the effects of extreme events in satellite images based on tensor decomposition learning.
- The proposed method can deal with multi-temporal multispectral images for change detection.
- The tensor learning model can simultaneously exploit the spatial and spectral features in the images with low complexity.
- Experimental results on real satellite images demonstrate the effectiveness of the proposed method.

2. TENSOR PRELIMINARIES

An N-way or Nth-order tensor $\mathcal{X} \in \mathbb{R}^{I_1 \times I_2 \times \cdots \times I_N}$ is defined as a multidimensional array, whereby the order of a tensor is the number of its dimensions. Tensors offer a mathematical way of representing and handling higher-order data using tensor decomposition techniques. Specifically, the Tucker decomposition involves expressing a tensor $\mathcal{X} \in \mathbb{R}^{I_1 \times I_2 \times \cdots \times I_N}$ as a core tensor $\mathcal{G} \in \mathbb{R}^{R_1 \times R_2 \times \cdots \times R_N}$ multiplied by a matrix $\mathbf{D}_n \in \mathbb{R}^{I_n \times R_n}$ along each mode, i.e., $\mathcal{X} = \mathcal{G} \times_1 \mathbf{D}_1 \times_2 \mathbf{D}_2 \times_3 \cdots \times_N \mathbf{D}_N$, where the mode-$n$ product $\times_n$ denotes the tensor-times-matrix operation. This product can also be expressed in a matrix-format as $\mathcal{Y} = (\mathcal{G} \times_n \mathbf{D}_n) \Leftrightarrow \mathbf{Y}_{(n)} = \mathbf{D}_n \cdot \mathbf{G}_{(n)}$, where $\mathbf{G}_{(n)} \in \mathbb{R}^{R_n \times \prod_{i \neq n} R_i}$ is the mode-n matricization or unfolding of $\mathcal{G}$ and it corresponds to a matrix with columns being the vectors obtained by fixing all indices of $\mathcal{G}$ except the n-th index. The N-tuple $(R_1, R_2, ..., R_N)$ that corresponds to the dimensions of the core tensor in the exact Tucker decomposition with orthogonal factor matrices is called the multi-linear rank of $\mathcal{X} \in \mathbb{R}^{I_1 \times I_2 \times \cdots \times I_N}$. Specifically, the multi-linear rank indicates the rank of each mode matricization $\mathbf{X}_{(n)}$ of the tensor, for n=1, .., N with $R_n \leq I_n$.

3. PROPOSED METHOD

The proposed change detection method which is illustrated in Fig. 1, consists of the training and the run-time phases, implemented on small patches of the images.

Training Phase

Given a set of training satellite multispectral image patches $\mathcal{X}^j \in \mathbb{R}^{H \times W \times B}$, with two spatial and one spectral dimension, we can obtain the training tensor $\mathcal{X} = (\mathcal{X}^1, \mathcal{X}^2, ..., \mathcal{X}^S) \in \mathbb{R}^{H \times W \times B \times S}$, where S is the number of training samples.

To obtain the feature space of the training samples, we learn a basis for each dimension, $\mathbf{D}_H, \mathbf{D}_W, \mathbf{D}_B$, such that each sample can be written as a multilinear combination of them, i.e., $\mathcal{X}^j = \mathcal{G}^j \times_1 \mathbf{D}_H \times_2 \mathbf{D}_W \times_3 \mathbf{D}_B$, for $j = 1, .., S$.

To achieve this, we minimize the error between the training tensor and its Tucker decomposition subject to a low-rank constraint on the factor matrix of the sample-variable $\mathbf{D}_S$ to extract the correlations in the training data, and an orthogonality constraint on the other factor matrices to obtain an orthogonal basis along each mode. Specifically, we solve the optimization problem

$$\begin{gathered}\min \tfrac{1}{2}\|\mathcal{X}-\mathcal{G}\times_1\mathbf{D}_H\times_2\mathbf{D}_W\times_3\mathbf{D}_B\times_4\mathbf{D}_S\|_F^2+\lambda\|\mathbf{A}\|_* \\ \text{subject to } \mathbf{A}=\mathbf{D}_S,\ \mathbf{D}_n^T\cdot\mathbf{D}_n=\mathbf{I}_{R_n},\ n=H,W,B\end{gathered} \tag{1}$$

where $\mathcal{G}\in\mathbb{R}^{R_H\times R_W\times R_B\times S}$, $\mathbf{D}_H\in\mathbb{R}^{H\times R_H}$, $\mathbf{D}_W\in\mathbb{R}^{W\times R_W}$, $\mathbf{D}_B\in\mathbb{R}^{B\times R_B}$, with $R_H\leq H$, $R_W\leq W$, and $R_B\leq B$, $\mathbf{D}_S,\mathbf{A}\in\mathbb{R}^{S\times S}$, $\mathbf{I}_{R_n}$ is the identity matrix with dimensions $R_n\times R_n$, and the parameter $\lambda>0$ is used to control the terms of the optimization problem.

To solve this problem, we apply the Alternating Direction Method of Multipliers, in which we minimize the augmented Lagrangian function $\mathcal{L}$ iteratively for each variable while keeping the others fixed, where

$$\begin{gathered}\mathcal{L}(\mathcal{G},\mathbf{D}_H,\mathbf{D}_W,\mathbf{D}_B,\mathbf{D}_S,\mathbf{A},\mathbf{Y})= \\ \tfrac{1}{2}\|\mathcal{X}-\mathcal{G}\times_1\mathbf{D}_H\times_2\mathbf{D}_W\times_3\mathbf{D}_B\times_4\mathbf{D}_S\|_F^2+\lambda\|\mathbf{A}\|_*+ \\ \mathbf{Y}\cdot(\mathbf{A}-\mathbf{D}_S)+\tfrac{p}{2}\|\mathbf{A}-\mathbf{D}_S\|_F^2,\end{gathered} \tag{2}$$

$\mathbf{Y}\in\mathbb{R}^{S\times S}$ stands for the Lagrange multiplier matrix, and $p>0$ denotes the step size parameter. Specifically, at each iteration l, we update the auxiliary variable $\mathbf{A}$ as

$$\hat{\mathbf{A}}\leftarrow\mathbf{D}_S-\frac{\mathbf{Y}}{p}. \tag{3}$$

and we hold some of its singular values obtained from the Singular Value Decomposition, depending on the parameter λ (90% of the information of the singular values in our experiments) to impose the nuclear norm constraint on it.
For the basis matrices $\mathbf{D}_n, n=H,W,B$, we update

$$\hat{\mathbf{D}}_n \leftarrow (\mathbf{X}_{(n)}\cdot\mathbf{C}_{n_{(n)}}^T)\cdot(\mathbf{C}_{n_{(n)}}\cdot\mathbf{C}_{n_{(n)}}^T)^{-1} \tag{4}$$

$$(\mathbf{Q},\mathbf{R}) \leftarrow QR(\hat{\mathbf{D}}_n) \tag{5}$$

$$\mathbf{D}_n \leftarrow \mathbf{Q}(:,1:R_n), \tag{6}$$

where $\mathcal{C}_n=\mathcal{G}\times_1\cdots\times_{n-1}\mathbf{D}_{n-1}\times_{n+1}\mathbf{D}_{n+1}\times_{n+2}\cdots$, and the *QR* factorization is applied to impose the orthogonality constraint on them.
The update of the other variables is more straightforward since there is no constraint on them, i.e., we update

$$\begin{aligned}\mathbf{D}_S \leftarrow\ & (\mathbf{X}_{(S)}\cdot\mathbf{C}_{S_{(S)}}^T+\mathbf{Y}+p\cdot\mathbf{A})\cdot \\ & \cdot(\mathbf{C}_{S_{(S)}}\cdot\mathbf{C}_{S_{(S)}}^T+p\cdot\mathbf{I}_S)^{-1}\end{aligned} \tag{7}$$

$$\mathcal{G} \leftarrow \mathcal{X}\times_1\mathbf{D}_H^T\times_2\mathbf{D}_W^T\times_3\mathbf{D}_B^T\times_4\mathbf{D}_S^{-1} \tag{8}$$

$$\mathbf{Y}^{(l)} \leftarrow \mathbf{Y}^{(l-1)}+p\cdot(\mathbf{A}-\mathbf{D}_S), \tag{9}$$

at each iteration l, where $\mathbf{D}_n^{-1}=\mathbf{D}_n^T$ and $\mathbf{D}_n^T\cdot\mathbf{D}_n=\mathbf{I}_{R_n}$ for the orthogonal matrices $\mathbf{D}_n, n=H,W,B$, and $p=0.01$.

Note that we first introduced the tensor decomposition learning method for the compression of high-dimensional signals [19]. Nevertheless, this tensor learning model can be effectively employed for the unsupervised change detection problem. In this task, the objective is to reconstruct the original data while simultaneously acquiring a representative feature space representation. Because the feature space has lower dimensionality in comparison to the original data, it can be viewed as a compressed space. This compressed space retains only the distinguishing features in the representation, offering robustness to noise and requiring less computational and memory resources. This aspect is crucial in remote sensing applications.

Run-time Phase

During inference, a time series of multispectral satellite images is given that consists of a number F of history frames before an extreme event and an image after the event of the same location. Each patch $\hat{\mathcal{X}}_f\in\mathbb{R}^{H\times W\times B}, f=1,..,F+1$ in the image time series is represented in the feature space by expressing it as a multilinear combination of the learned basis matrices $\mathbf{D}_H,\mathbf{D}_W,\mathbf{D}_B$. Specifically, the extracted features are encoded in the core tensor of coefficients by calculating the mode-n product of the image patch with the transposed basis matrices, i.e.,

$$\hat{\mathcal{G}}_f=\hat{\mathcal{X}}_f\times_1\mathbf{D}_H^T\times_2\mathbf{D}_W^T\times_3\mathbf{D}_B^T. \tag{10}$$

To detect the changes in each patch of the images before and after the event, we compare the corresponding features using the score function $S:\mathbb{R}^{R_H\times R_W\times R_B\times(F+1)}\rightarrow\mathbb{R}$ defined as

$$S(\hat{\mathcal{G}})=\min_{f=1,..F} d(\hat{\mathcal{G}}_f,\hat{\mathcal{G}}_{F+1}). \tag{11}$$

Therefore, the predicted scores are obtained as the minimum value of the distances between the features of the history frames before the event and the features of the frame after the event, using as distance metric the Spectral Angle Mapper (SAM) [20]. As the proposed change detection method operates on small image patches, a score is extracted for each patch to determine whether the pixels within that patch have undergone changes. This is achieved by applying a threshold. Hence, operating on small patches can reduce the error in case there are changed and unchanged pixels in a patch. Moreover, the utilization of the minimum in the score function allows us to handle multi-temporal data effectively, aggregating individual distances while disregarding minor fluctuations.

4. EXPERIMENTAL RESULTS

To assess the suggested change detection method, we initially trained our tensor decomposition learning model using 100 Sentinel-2 multispectral images with dimensions $30\times30\times10$. The model utilized the ten highest resolution spectral bands. Additionally, we implemented the proposed method on spatial patches with dimensions of 3×3. We employed a multilinear rank of 1 for the spatial dimensions to capture spatial

correlations, and a full rank for the spectral dimension allowing us to leverage all available spectral information. In this context, the multilinear rank corresponds to the size of the learned feature space.

During inference, we performed experiments on the RaVÆn dataset [18] for the detection of the effects of fires and floods in multi-temporal Sentinel-2 images. Specifically, there are 5 different locations of fires and 4 locations of floods. Every location comprises a time series containing five images. The initial four images are captured before the disaster occurs, while the fifth image is taken afterward. Importantly, each of these images exhibits less than 20% cloud cover. To mitigate the impact of clouds on the outcomes, we opted for frames with lower cloud cover in each time series during our experiments. A change mask representing the actual differences between the last two images in the time series is also provided, solely for evaluation purposes.

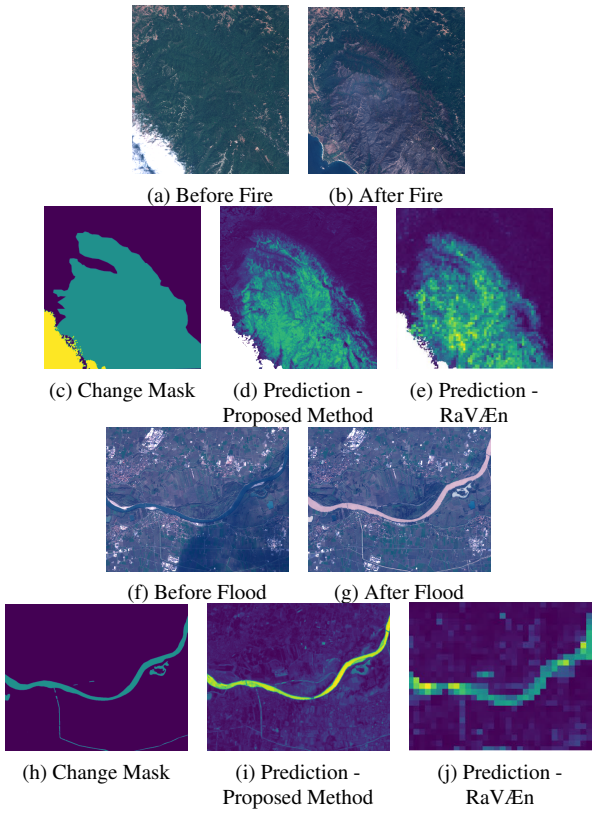

(a) Before Fire (b) After Fire

(c) Change Mask (d) Prediction - Proposed Method (e) Prediction - RaVÆn

(f) Before Flood (g) After Flood

(h) Change Mask (i) Prediction - Proposed Method (j) Prediction - RaVÆn

Fig. 2: The images before and after the fire and flood and the corresponding predicted scores of the proposed and the competing method in comparison with the true change mask.

To evaluate the proposed unsupervised change detection method of multi-temporal satellite images, we compared it with the RaVÆn method [18]. Specifically, the mean Area Under Precision-Recall Curve (AUPRC) is reported in Table 1 for both methods on each extreme event, using 1 and 3 history frames and performing 5 Monte-Carlo simulations. As observed, the proposed approach consistently surpasses the competing method in every case, delivering more reliable results with minimal standard deviation across the randomness of the simulations. The effectiveness of the proposed method is further confirmed by examining the images displaying the predicted scores of both methods, as illustrated in Fig. 2. The comparison is made with the true change mask, focusing on the affected area of each event.

Table 1: Comparison of the proposed method with RaVÆn on each extreme event, using 1 and 3 history frames.

AUPRC	History	Fires	Floods
Proposed Method	1	**0.939** ($1.71 \cdot 10^{-10}$)	**0.764** ($8.78 \cdot 10^{-9}$)
	3	**0.937** ($1.91 \cdot 10^{-10}$)	**0.741** ($5.18 \cdot 10^{-9}$)
RaVÆn	1	0.833 (0.008)	0.448 (0.011)
	3	0.913 (0.008)	0.443 (0.009)

We also examined the impact of the number of history frames on the change detection results in Table 2 on a location affected by floods. As it was expected, we can obtain more accurate predictions using more history frames since more information can be extracted from the images before the event. Note here that we selected a region without clouds in the images of the time series. However, many images in the dataset have cloud cover regions that prevent the appropriate feature extraction from the history frames. This is the reason that the results of our method are not improved in the case of 3 history frames instead of 1, as we can see in Table 1.

Table 2: AUPRC of our method concerning different numbers of history frames on a location affected by floods.

AUPRC	Number of history frames			
	1	2	3	4
Proposed Method	0.8124 ($3.56{\cdot}10^{-8}$)	0.9327 ($4.54{\cdot}10^{-9}$)	0.9441 ($5.34{\cdot}10^{-9}$)	0.9563 ($7.89{\cdot}10^{-9}$)

Finally, an important characteristic of the proposed model is the low complexity since it only requires $3{\cdot}1{+}3{\cdot}1{+}10{\cdot}10 = 106$ parameters (i.e., the number of elements in the 3 basis matrices) for the representation of the feature space obtained during tensor decomposition learning. However, the alternative method involves approximately a million parameters, leading to a substantial increase in computational and memory requirements. This aspect is particularly crucial in remote sensing scenarios.

5. CONCLUSION

This work introduced an unsupervised method for detecting changes during extreme events in multi-temporal satellite images. The approach utilizes tensor decomposition learning to extract the feature space, effectively incorporating spatial and spectral features with low complexity. The changed pixels are obtained by comparing the extracted features of the images before and after the event, using the learned factors. Our future work involves applying the proposed method to additional extreme events with a greater number of historical frames.

6. REFERENCES

[1] Jungho Im, Haemi Park, and Wataru Takeuchi, "Advances in remote sensing-based disaster monitoring and assessment," 2019.

[2] John Rogan and DongMei Chen, "Remote sensing technology for mapping and monitoring land-cover and land-use change," *Progress in planning*, vol. 61, no. 4, pp. 301–325, 2004.

[3] Lorenzo Bruzzone and Diego F Prieto, "Automatic analysis of the difference image for unsupervised change detection," *IEEE Transactions on Geoscience and Remote sensing*, vol. 38, no. 3, pp. 1171–1182, 2000.

[4] Zeki Yetgin, "Unsupervised change detection of satellite images using local gradual descent," *IEEE Transactions on Geoscience and Remote Sensing*, vol. 50, no. 5, pp. 1919–1929, 2011.

[5] Ming Hao, Wenzhong Shi, Hua Zhang, and Chang Li, "Unsupervised change detection with expectation-maximization-based level set," *IEEE Geoscience and Remote Sensing Letters*, vol. 11, no. 1, pp. 210–214, 2013.

[6] Sicong Liu, Qian Du, Xiaohua Tong, Alim Samat, and Lorenzo Bruzzone, "Unsupervised change detection in multispectral remote sensing images via spectral-spatial band expansion," *IEEE Journal of Selected Topics in Applied Earth Observations and Remote Sensing*, vol. 12, no. 9, pp. 3578–3587, 2019.

[7] Youxi He, Zhenhong Jia, Jie Yang, and Nikola K Kasabov, "Multispectral image change detection based on single-band slow feature analysis," *Remote Sensing*, vol. 13, no. 15, pp. 2969, 2021.

[8] Walma Gharbi, Lotfi Chaâri, and Amel Benazza-Benyahia, "Unsupervised bayesian change detection for remotely sensed images," *Signal, Image and Video Processing*, vol. 15, pp. 205–213, 2021.

[9] Hyeoncheol Noh, Jingi Ju, Minseok Seo, Jongchan Park, and Dong-Geol Choi, "Unsupervised change detection based on image reconstruction loss," in *Proceedings of the IEEE/CVF Conference on Computer Vision and Pattern Recognition*, 2022, pp. 1352–1361.

[10] Kevin Louis de Jong and Anna Sergeevna Bosman, "Unsupervised change detection in satellite images using convolutional neural networks," in *2019 International joint conference on neural networks (IJCNN)*. IEEE, 2019, pp. 1–8.

[11] Bo Du, Lixiang Ru, Chen Wu, and Liangpei Zhang, "Unsupervised deep slow feature analysis for change detection in multi-temporal remote sensing images," *IEEE Transactions on Geoscience and Remote Sensing*, vol. 57, no. 12, pp. 9976–9992, 2019.

[12] Luca Bergamasco, Sudipan Saha, Francesca Bovolo, and Lorenzo Bruzzone, "An explainable convolutional autoencoder model for unsupervised change detection," *The International Archives of the Photogrammetry, Remote Sensing and Spatial Information Sciences*, vol. 43, pp. 1513–1519, 2020.

[13] Caijun Ren, Xiangyu Wang, Jian Gao, Xiren Zhou, and Huanhuan Chen, "Unsupervised change detection in satellite images with generative adversarial network," *IEEE Transactions on Geoscience and Remote Sensing*, vol. 59, no. 12, pp. 10047–10061, 2020.

[14] Ekaterina Kalinicheva, Dino Ienco, Jérémie Sublime, and Maria Trocan, "Unsupervised change detection analysis in satellite image time series using deep learning combined with graph-based approaches," *IEEE Journal of Selected Topics in Applied Earth Observations and Remote Sensing*, vol. 13, pp. 1450–1466, 2020.

[15] Nicholas D Sidiropoulos, Lieven De Lathauwer, Xiao Fu, Kejun Huang, Evangelos E Papalexakis, and Christos Faloutsos, "Tensor decomposition for signal processing and machine learning," *IEEE Transactions on signal processing*, vol. 65, no. 13, pp. 3551–3582, 2017.

[16] Zengfu Hou, Wei Li, Ran Tao, and Qian Du, "Three-order tucker decomposition and reconstruction detector for unsupervised hyperspectral change detection," *IEEE Journal of Selected Topics in Applied Earth Observations and Remote Sensing*, vol. 14, pp. 6194–6205, 2021.

[17] Muhammad Sohail, Haonan Wu, Zhao Chen, and Guohua Liu, "Unsupervised and self-supervised tensor train for change detection in multitemporal hyperspectral images," *Electronics*, vol. 11, no. 9, pp. 1486, 2022.

[18] Vít Růžička, Anna Vaughan, Daniele De Martini, James Fulton, Valentina Salvatelli, Chris Bridges, Gonzalo Mateo-Garcia, and Valentina Zantedeschi, "Ravæn: unsupervised change detection of extreme events using ml on-board satellites," *Scientific reports*, vol. 12, no. 1, pp. 16939, 2022.

[19] Anastasia Aidini, Grigorios Tsagkatakis, and Panagiotis Tsakalides, "Tensor decomposition learning for compression of multidimensional signals," *IEEE Journal of Selected Topics in Signal Processing*, vol. 15, no. 3, pp. 476–490, 2021.

[20] Chenghai Yang, James H Everitt, and Joe M Bradford, "Yield estimation from hyperspectral imagery using spectral angle mapper (sam)," *Transactions of the ASABE*, vol. 51, no. 2, pp. 729–737, 2008.